Energy Detection based Spectrum Sensing over Two-wave with Diffuse Power Fading Channels

Eleftherios Chatziantoniou, *Member, IEEE*, Ben Allen, *Senior Member, IEEE*, Vladan Velisavljevic, *Senior Member, IEEE*, Petros Karadimas, *Member, IEEE*, Justin Coon, *Senior Member, IEEE*

***Abstract*—One of the most important factors that affects the performance of energy detection (ED) is the fading channel between the wireless nodes. This article investigates the performance of ED-based spectrum sensing, for cognitive radio (CR), over two-wave with diffuse power (TWDP) fading channels. The TWDP fading model characterizes a variety of fading channels, including well-known canonical fading distributions, such as Rayleigh and Rician, as well as worse than Rayleigh fading conditions modeled by the two-ray fading model. Novel analytic expressions for the average probability of detection over TWDP fading that account for single-user and cooperative spectrum sensing as well as square law selection diversity reception are derived. These expressions are used to analyze the behavior of ED-based spectrum sensing over moderate, severe and extreme fading conditions, and to investigate the use of cooperation and diversity as a means of mitigating the fading effects. The obtained results indicate that TWDP fading conditions can significantly degrade the sensing performance; however, it is shown that detection performance can be improved when cooperation and diversity are employed. The presented outcomes enable identifying the limits of ED-based spectrum sensing and quantifying the trade-offs between detection performance and energy efficiency for cognitive radio systems deployed within confined environments such as in-vehicular wireless networks.**

***Index Terms*—Cognitive radio (CR), cooperative spectrum sensing, diversity reception, energy detection (ED), noise uncertainty, spectrum sensing, two-wave with diffuse power (TWDP) fading**

I. Introduction

ENERGY DETECTION (ED), is a non-coherent detection method that measures the energy level of an unknown received signal and compares it with a predefined threshold in order to determine its presence or absence within a given bandwidth. The problem of detecting unknown deterministic signals over flat band-limited Gaussian channels was first considered by Urkowitz in [1]. The detection of signals of random amplitude including Rayleigh, Rician and Nakagami distributions was studied by Kostylev in [2]. ED has been widely used in a variety of wireless applications such as RADAR systems and ultra-wideband communications [3]. Owing to its simplicity and no need for prior knowledge on the received signal, ED is considered as the most viable spectrum sensing method for cognitive radio (CR) [4]. CR technology has been proposed as a means of improving spectrum utilization by allowing unlicensed secondary users (SUs) to dynamically access the licensed radio spectrum without interfering with the primary users (PUs) [5]. This can be achieved by using CR-enabled radios that sense their spectral environment and adapt their transmission parameters according to the PU spectrum occupancy statistics [6]. In this context, ED is used as a spectrum sensing mechanism in order for SUs to determine whether a PU is present or absent in a given frequency band.

The detection performance of ED-based spectrum sensing is significantly influenced by the fading channel between the SU and PU wireless nodes. Therefore, the performance of ED-based spectrum sensing has been studied for a variety of fading channels such as Rayleigh, Rician and Nakagami [7]. In [8], the performance of ED over Nakagami-m fading has been evaluated. Likewise, the detection of unknown signals over K-distributed and generalized K fading channels has been analyzed in [9]. Furthermore, the behavior of ED-based spectrum sensing over κ-μ and κ-μ extreme fading channels has been recently investigated in [10]. All aforementioned studies focus on the performance of ED-based spectrum sensing over traditional fading channels for conventional outdoor and indoor propagation scenarios. However, as wireless technology evolves, CR is expected to be applied in support of emerging applications such as Machine-to-Machine (M2M) communications and wireless sensor networks (WSN) as a practical realization of the Internet-of-Things concept [11], [12].

Compared to traditional wireless systems, M2M communications introduce a new wireless landscape, where wireless nodes operate within non-conventional environments. Such environments have been found to exhibit fading conditions that are not effectively described by existing fading models. Indicatively, WSNs deployed in cavity environments (e.g. aircraft, public transportation vehicles), vehicle-to-vehicle communications and enclosed structures (e.g. inside computer cabinets) have been found to exhibit frequency-dependent and spatially-dependent fading whose severity exceeds those predicted by the Rayleigh fading model [13], [14]. Such small-scale fading conditions, termed as "hyper-Rayleigh", were experimentally verified to be adequately characterized by the two-wave with diffuse power (TWDP) model [15]. The TWDP model has been recently considered for CR in [16], in which a method for determining the optimal detection threshold for ED-based spectrum sensing over "hyper-Rayleigh" fading is proposed. However, this method considers only single user spectrum sensing and is limited for the case of a time-bandwidth product equal to 1.

In this article an analytic expression for the average probability of detection for ED-based spectrum sensing over TWDP fading channels, which can be validated for any positive time-bandwidth product value, is derived. This expression is extended to account for cooperative spectrum sensing and

square law selection (SLS) diversity reception to mitigate the effects of fading and improve the sensing performance over TWDP fading channels. The presented results provide a new insight into the performance of ED over worse than Rayleigh fading conditions that can describe the behavior of ED-based spectrum sensing over fading conditions that occur within non-traditional propagation environments such as metallic enclosed structures. The derived expressions can form the basis of analyzing the performance and designing future CR systems for emerging wireless applications such as cognitive M2M communication systems and in-vehicular wireless sensor networks.

The remainder of this article is organized as follows. Section II presents the fundamentals of ED and describes the theoretical underpinnings of the TWDP fading model. In Section III, analytic expressions for the average probability of detection for single user and cooperative spectrum sensing as well as for an SLS diversity reception scheme are derived. Numerical results and discussion for different fading scenarios are provided in Section IV. The conclusions of this work are presented in Section V.

II. System and Channel Model

A. Energy Detection Fundamentals

In the context of a wireless communications link, the received signal, $y(t)$, can be mathematically described as,

$$x(t) = hs(t) + n(t), \tag{1}$$

where $s(t)$ is the transmitted signal, h denotes the channel gain, $n(t)$ is additive white Gaussian noise (AWGN) and t is the time index.

For ED, the received signal is filtered within a bandwidth W, squared, and integrated over an observation interval T. The output of the integrator is the received signal's energy which is then used as a test statistic [1]. By comparing the test statistic, y, with a predefined detection threshold, λ, the detector has to distinguish between the following hypotheses,

$$x(t) = \begin{cases} n(t) & ,H_0 \\ hs(t) + n(t) & ,H_1, \end{cases} \tag{2}$$

where H_0 and H_1 denote the hypothesis of the signal to be absent or present, respectively. Given the time-bandwidth product, $u = TW$, the test statistic follows a central chi-square distribution with $2u$ degrees of freedom under hypothesis H_0 and a non-central chi-square distribution with $2u$ degrees of freedom under hypothesis H_1 [1]. As a result, the corresponding probability density function (PDF) of the test statistic y is given by [7],

$$f_y(y) = \begin{cases} \frac{1}{2^u \Gamma(u)} y^{u-1} e^{-\frac{y}{2}} & ,H_0 \\ \frac{1}{2}\frac{y}{2\gamma}^{\frac{u-1}{2}} e^{-\frac{y+2\gamma}{2}} I_{u-1}(\sqrt{2y\gamma}) & ,H_1, \end{cases} \tag{3}$$

where γ denotes the instantaneous signal-to-noise ratio (SNR), $\Gamma(a) = \int_0^\infty t^{a-1} e^{-t} dt$ is the Gamma function and $I_n(x) = (1/\pi) \int_0^\pi cos(n\theta) e^{xcos(\theta)} d\theta$ is the modified Bessel function of the first kind [17].

The sensing performance of ED is evaluated in terms of the probability of false alarm P_{fa}, (i.e. false positive rate of signal detection), probability of detection, P_d, (i.e. true positive rate of signal detection), and probability of missed detection, $P_{md} = 1 - P_d$, (i.e. false negative rate of signal signal detection).

By integrating (3) over the limits of zero to infinity, P_{fa} and P_d are obtained as [7],

$$P_{fa} = \frac{\Gamma(u, \lambda/2)}{\Gamma(u)} \tag{4}$$

$$P_d = Q_u(\sqrt{2\gamma}, \sqrt{\lambda}), \tag{5}$$

where $\Gamma(a, x) = \int_x^\infty t^{(a-t)} e^{-t} dt$ and $Q_m(a, b) = (1/a^{(m-1)}) \int_b^\infty x^m e^{-(x^2+a^2)/2} I_{(m-1)}(ax) dx$ denote the incomplete gamma function and the generalized Marcum Q-function, respectively [17], [18].

B. TWDP fading Model

Durgin et. al derived a new parametric family of PDFs that approximates the TWDP PDF and describes small-scale fading in the presence of two multipath components [19]. This family of PDFs can characterize a variety of fading scenarios including those experienced by narrow-band receivers, the use of directional antennas, and wide-band signals. In addition, the TWDP fading model has been found to be particularly versatile since it reduces to the well-known Rician and Rayleigh distributions.

The TWDP PDF can be entirely described by two physically intuitive parameters of the wireless channel [19]: 1) the ratio of the specular components' power to the diffuse power , given as $K = (V_1^2 + V_2^2)/2\sigma^2$, where V_1 and V_2 denote the voltage magnitudes of the two specular waves, and $2\sigma^2$ represents the average power of the diffuse waves; 2) the relative strength of the two specular waves expressed as $\Delta = 2V_1V_2/(V_1^2 + V_2^2)$. According to [19], the approximate PDF of the fading envelope, r, is given as,

$$f_r(r) = \frac{r}{\sigma^2} e^{\left(-\frac{r^2}{2\sigma^2} - K\right)} \sum_{i=1}^{M} a_i D\left(\frac{r}{\sigma}; K; a_i\right), \tag{6}$$

where,

$$\begin{aligned} D(x; K; a) =& \frac{1}{2} e^{aK} I_0\left(x\sqrt{2K(1-a)}\right) \\ &+ \frac{1}{2} e^{-aK} I_0\left(x\sqrt{2K(1+a)}\right), \end{aligned} \tag{7}$$

where a_i is the approximation coefficient, M represents the order of approximation of the TWDP PDF and $I_0(.)$ denotes the zero-order Bessel function of the first kind. The minimum required approximation order, M, is determined by the product of the fading parameters K and Δ as $M_{min} \geq \lceil 1/2K\Delta \rceil$, with $\lceil . \rceil$ denoting the ceiling function.

In two special cases, the TWDP PDF degenerates to the Rician PDF when $K \neq 0$ and $\Delta = 0$, and to the Rayleigh PDF when $K = 0$. Furthermore, for $K \to \infty$ and $\Delta = 1$ the TWDP PDF reduces to the two-ray PDF, which represents a fading channel that consists of two summed multipath components of equal weights. Such fading conditions, over which the envelope statistics are no longer Rayleigh distributed have

been experimentally validated as worse than Rayleigh fading in [15].

Given the PDF of the envelope over a TWDP fading channel in (6) and that $\gamma = \bar{\gamma}/2\sigma^2(K+1)$, the corresponding PDF of the SNR can be obtained by performing a squared transformation of the random variable r, in (6) [20]. Formally,

$$f_\gamma(\gamma) = \frac{K+1}{2\bar{\gamma}} e^{-K} \sum_{i=1}^{M} a_i \Bigg[e^{a_i K} e^{-\frac{(K+1)\gamma}{\bar{\gamma}}} Z(a_i) + e^{-a_i K} e^{-\frac{(K+1)\gamma}{\bar{\gamma}}} Z(-a_i) \Bigg], \tag{8}$$

where,

$$Z(\pm a_i) = I_0 \left(2\sqrt{\frac{K(K+1)(1 \pm a_i)\gamma}{\bar{\gamma}}} \right), \tag{9}$$

with $\bar{\gamma}$ denoting the average SNR.

III. Energy Detection Over TWDP Fading Channels

A. Single User Spectrum Sensing

In a fading channel, where the channel gain, h, varies, the average probability of detection, $\bar{P}_d$, is obtained by averaging the probability of detection for a non-fading AWGN channel over the corresponding SNR fading statistics [21]. Formally,

$$\bar{P}_d = \int_0^\infty Q_u(\sqrt{2\gamma}, \sqrt{\lambda}) f_\gamma(\gamma)\, d\gamma \ . \tag{10}$$

By substituting (8) into (10) the average probability of detection over TWDP, $\bar{P}_{d_{TWDP}}$, is obtained as,

$$\bar{P}_{d_{TWDP}} = \int_0^\infty Q_u(\sqrt{2\gamma}, \sqrt{\lambda}) \frac{K+1}{2\bar{\gamma}} e^{-K} \times \sum_{i=1}^{M} \left[e^{a_i K} e^{-\frac{(K+1)\gamma}{\bar{\gamma}}} Z(-a_i) + e^{-a_i K} e^{-\frac{(K+1)\gamma}{\bar{\gamma}}} Z(a_i) \right] d\gamma \ . \tag{11}$$

An analytic expression for (11) can be derived by using an infinite series representation of the Marcum Q-function. By using [22, eq. (27)], (5) can be expressed as a sum of n terms,

$$P_d = e^{-\frac{\lambda}{2}} \sum_{l=0}^{u-1} \frac{\left(\frac{\lambda}{2}\right)^l}{l!} + e^{-\frac{\lambda}{2}} \sum_{n=u}^{\infty} \frac{\left(\frac{\lambda}{2}\right)^n}{n!} \left(1 - e^{-\gamma} \sum_{k=0}^{n-u} \frac{\gamma^k}{k!} \right). \tag{12}$$

By substituting (12) into (11), $\bar{P}_{d_{TWDP}}$ is obtained as,

$$\bar{P}_{d_{TWDP}} = e^{-\frac{\lambda}{2}} \sum_{l=0}^{u-1} \frac{\left(\frac{\lambda}{2}\right)^l}{l!} + e^{-\frac{\lambda}{2}} \sum_{n=u}^{\infty} \frac{\left(\frac{\lambda}{2}\right)^n}{n!} \left(1 - \frac{(K+1)e^{-K}}{2\bar{\gamma}} \sum_{k=0}^{n-u} \sum_{i=1}^{M} \frac{\int_0^\infty \gamma^k [e^{a_i K} e^{-\frac{K+\bar{\gamma}+1}{\bar{\gamma}}\gamma} Z(-a_i) + e^{-a_i K} e^{-\frac{K+\bar{\gamma}+1}{\bar{\gamma}}\gamma} Z(a_i)] d\gamma}{k!} \right). \tag{13}$$

Expression (13) involves $2M$ integrals of the same form, which can be calculated by using [23, eq. (6.643-2)]. With the aid of the Whittaker function identity [23, eq. (9.220-2)] and after some algebraic manipulations an analytic expression for $\bar{P}_{d_{TWDP}}$ is derived in (14), shown in the footnote, where $\Phi(\alpha;\beta;z)$ denotes the Confluent Hypergeometric function, which is available in most of commonly used mathematical software packages such as MATLAB and MATHEMATICA [23]. The derivation of (14) is described in the Appendix.

In order to evaluate (14), truncation of the infinite series is required. The upper bound for the truncation error of (14) using N terms is given as [22, eq. (28)],

$$|E| \leq 1 - e^{-\frac{\lambda}{2}} \sum_{n=0}^{u+N} \frac{\left(\frac{\lambda}{2}\right)^n}{n!} \left(1 - \frac{(K+1)e^{-K}}{2(K+\bar{\gamma}+1)} \sum_{k=0}^{N+1} \sum_{i=1}^{M} e^{a_i K} \left(\frac{\bar{\gamma}}{K+\bar{\gamma}+1} \right)^k \Phi\left(k+1; 1; \frac{K(K+1)(1-a_i)}{K+\bar{\gamma}+1} \right) + e^{-a_i K} \left(\frac{\bar{\gamma}}{K+\bar{\gamma}+1} \right)^k \Phi\left(k+1; 1; \frac{K(K+1)(1+a_i)}{K+\bar{\gamma}+1} \right) \right). \tag{15}$$

Note that by using the infinite series representation in (14), $0 \leq P_{d_{TWDP}} \leq 1$. Hence, the sum of a finite number of terms, N, $0 \leq P_d^{(N)} \leq 1$. With $|E| = |P_d^{(N)} - P_d^{(N-1)}|$ denoting the truncation error, it can be seen that $|P_d^{(N)}| = |P_d^{(N-1)} + E| \leq 1$. Table I illustrates the minimum number of terms required to obtain a five figure accuracy when evaluating (14) for $K = 10$ dB and $\Delta = 1$ for a combination of different SNR and time-bandwidth product values, u.

B. Cooperative Spectrum Sensing

In many cases the detection performance of ED-based spectrum sensing is affected by destructive channel conditions since the CR terminals are unable to distinguish between an unoccupied channel and one that is attenuated by deep fading.

$$\bar{P}_{d_{TWDP}} = e^{-\frac{\lambda}{2}} \sum_{l=0}^{u-1} \frac{\left(\frac{\lambda}{2}\right)^l}{l!} + e^{-\frac{\lambda}{2}} \sum_{n=u}^{\infty} \frac{\left(\frac{\lambda}{2}\right)^n}{n!} \left(1 - \frac{(K+1)e^{-K}}{2(K+\bar{\gamma}+1)} \sum_{k=0}^{n-u} \sum_{i=1}^{M} e^{a_i K} \left(\frac{\bar{\gamma}}{K+\bar{\gamma}+1} \right)^k \times \Phi\left(k+1; 1; \frac{K(K+1)(1-a_i)}{K+\bar{\gamma}+1} \right) + e^{-a_i K} \left(\frac{\bar{\gamma}}{K+\bar{\gamma}+1} \right)^k \Phi\left(k+1; 1; \frac{K(K+1)(1+a_i)}{K+\bar{\gamma}+1} \right) \right) \tag{14}$$

TABLE I
NUMBER OF REQUIRED TERMS, N, IN ORDER FOR (15) TO ACHIEVE A TRUNCATION ERROR, $|E| \leq 10^{-5}$, FOR $P_{fa} = 0.1$, $K = 10\,dB$ AND $\Delta = 1$.

SNR (dB)	u=1	u=10	u=100
0	11	14	19
5	15	17	22
10	21	29	35

Cooperative spectrum sensing that exploits the spatial diversity among SUs to alleviate the effects of shadowing and multipath has been proposed as a means of improving the detection performance [24], [25]. For such a cooperative spectrum sensing scheme with m collaborative SUs, the probabilities of false alarm, Q_{fa} and detection Q_d are given as [26],

$$Q_{fa} = 1 - (1 - P_{fa})^m \tag{16}$$

$$Q_d = 1 - (1 - P_d)^m. \tag{17}$$

Hence, the probability of detection over TWDP fading of a CR system with m cooperative users, $Q_{d_{TWDP}}$, is obtained by substituting (14) into (17) resulting in an analytic expression given by (18) (see footnote). Given that Q_{fa} is independent of the fading statistics it can be evaluated as [7],

$$Q_{fa} = \left[\frac{\Gamma(u, \lambda/2)}{\Gamma(u)}\right]^m. \tag{19}$$

C. Spectrum Sensing with Diversity Reception

Diversity is a well known technique used to compensate for signal fades in wireless communication channels. SLS is an effective diversity reception scheme that is highly regarded due to its simplicity. Its principle is based on selecting the branch with the maximum decision statistic, i.e., $y_{SLS} = max[y_1, y_2, ...y_L]$ [27]. For an SLS diversity scheme with L independent and identically distributed (i.i.d) branches, the average probability of detection is given as [7],

$$\bar{P}_d^{SLS} = 1 - \prod_{j=1}^{L} \int_0^{\infty} \left[1 - Q_u(\sqrt{2\gamma_j}, \sqrt{\lambda}) f_{\gamma_j}(\gamma_j) d\gamma_j\right]. \tag{20}$$

Therefore, by substituting (14) into (20), an analytic expression for $\bar{P}_{d_{TWDP}}^{SLS}$ is given by (21), in the footnote. The corresponding probability of false alarm, P_{fa}^{SLS}, is independent of the fading statistics and thus, it can be evaluated as follows [7, eq. (14)],

$$P_{fa}^{SLS} = 1 - \prod_{j=1}^{L} \left[1 - \frac{\Gamma(u, \lambda/2)}{\Gamma(u)}\right]. \tag{22}$$

D. Noise Uncertainty

In all previous cases perfect noise estimation is assumed. However, due to the fact that ED is based on hypothesis-testing with statistical assumptions of noise such as linearity, Gaussianity, and stationarity, perfect noise estimation is not always possible in real-world scenarios. Therefore, assuming a noise uncertainty α, the estimated noise power, $\bar{\sigma}_w$, is modeled as $\bar{\sigma}_w \in [\sigma_w/\alpha, \alpha\sigma_w]$, where σ_w denotes the nominal noise power. Therefore, for the worst-case, $\bar{\sigma}_w = \alpha\sigma_w$, (5) becomes [28],

$$P_d = Q_u(\sqrt{2\gamma}, \alpha\sqrt{\lambda}). \tag{23}$$

Hence, by evaluating (23) over the TWDP SNR statistics using (8), as described in Section III.A, a closed-form expression for the average probability of detection over TWDP with noise uncertainty is obtained by scaling the detection threshold, λ, with the noise uncertainty term a, i.e., λ is replaced by $a\lambda$ in (14).

IV. NUMERICAL RESULTS AND DISCUSSION

This section analyzes the behavior of ED-based spectrum sensing over TWDP fading channels. The sensing performance is evaluated over different scenarios with respect to $\bar{P}_d$ versus SNR and in terms of both Receiver Operating Characteristics (ROC) (P_d versus P_{fa}) and complementary ROC (P_{md} versus P_{fa}) curves. Furthermore, the effect of the fading parameters on P_d in negative SNR regions is quantified. The considered fading scenarios have been selected to represent moderate, severe and worse than Rayleigh fading conditions within realistic operational environments. The accuracy of the derived expressions is validated through comparison of results obtained by Monte-Carlo simulations. The simulation model

$$\bar{Q}_{d_{TWDP}} = 1 - \left[1 - e^{-\frac{\lambda}{2}} \sum_{l=0}^{u-1} \frac{\left(\frac{\lambda}{2}\right)^l}{l!} + e^{-\frac{\lambda}{2}} \sum_{n=u}^{\infty} \frac{\left(\frac{\lambda}{2}\right)^n}{n!} \left(1 - \frac{(K+1)e^{-K}}{2(K+\bar{\gamma}+1)} \sum_{k=0}^{n-u} \sum_{i=1}^{M} e^{a_i K} \left(\frac{\bar{\gamma}}{K+\bar{\gamma}+1}\right)^k \times \Phi\left(k+1; 1; \frac{K(K+1)(1-a_i)}{K+\bar{\gamma}+1}\right) + e^{-a_i K} \left(\frac{\bar{\gamma}}{K+\bar{\gamma}+1}\right)^k \Phi\left(k+1; 1; \frac{K(K+1)(1+a_i)}{K+\bar{\gamma}+1}\right)\right]^m \tag{18}$$

$$\bar{P}_{d_{TWDP}}^{SLS} = 1 - \prod_{j=1}^{L} \left[1 - \left[e^{-\frac{\lambda}{2}} \sum_{l=0}^{u-1} \frac{\left(\frac{\lambda}{2}\right)^l}{l!} + e^{-\frac{\lambda}{2}} \sum_{n=u}^{\infty} \frac{\left(\frac{\lambda}{2}\right)^n}{n!} \left(1 - \frac{(K+1)e^{-K}}{2(K+\bar{\gamma}_j+1)} \sum_{k=0}^{n-u} \sum_{i=1}^{M} e^{a_i K} \left(\frac{\bar{\gamma}_j}{K+\bar{\gamma}_j+1}\right)^k \Phi\left(k+1; 1; \frac{K(K+1)(1-a_i)}{K+\bar{\gamma}_j+1}\right) + e^{-a_i K} \left(\frac{\bar{\gamma}_j}{K+\bar{\gamma}_j+1}\right)^k \Phi\left(k+1; 1; \frac{K(K+1)(1+a_i)}{K+\bar{\gamma}_j+1}\right)\right]\right] \tag{21}$$

generates the received signal at the detector's front-end based on (1). Given that the derived expressions are independent of modulation, no modulation is considered for the transmitted signal. Furthermore, owing to the non-coherent nature of ED, no synchronization between the PU and SU is required. The channel fading coefficients are obtained from the TWDP PDF (6), whereas the noise samples are drawn from a Gaussian distribution, $\mathcal{N}(0,1)$. The energy of the received signal is compared to the detection threshold in order to obtain the corresponding P_d and P_{fa} values, which are averaged over 10^6 iterations.

Fig. 1 shows the complementary ROC curve for ED-based spectrum sensing over TWDP fading for different K and Δ values with a target P_{fa} of 0.1, an average SNR of 15 dB and a time-bandwidth product, $u = 1$ [28]. The complementary ROC curves for Rician and Rayleigh fading channels are provided for comparison between the derived expression and the corresponding expressions from [7]. The good match between these curves and between the simulation and analytical results validate the flexibility of the derived expression to account for Rician and Rayleigh fading. It is observed that as the value of K increases, the ROC curve moves within the hyper-Rayleigh region towards the upper bound of two-ray fading ($K = \infty$, $\Delta = 1$). These results suggest that the cancellation of two anti-phase specular waves and the low power of the diffuse components results to inferior detection performance compared to Rayleigh fading. Indicatively, for a $P_{md} = 0.1$, i.e, $P_d = 0.9$ the corresponding P_{fa} is 0.01, 0.03 and 0.27, under Rician, Rayleigh and hyper-Rayleigh fading, respectively. Thus, the required criterion $P_{fa} \leq 0.1$ is not met over "hyper-Rayleigh" fading conditions, which in turn leads to low spectral utilization.

Fig. 2 describes the sensing performance for severe fading scenarios where the diffuse components are of equal power and the total power of the specular waves is at least ten times that of the diffuse component. Under such fading conditions, as the value K increases, the product of K and Δ becomes large and the TWDP PDF becomes bimodal, thus exhibiting two maxima [19]. This results in the order change that is observed in the $\bar{\gamma}$ versus $\bar{P}_{d_{TWDP}}$ curves at an SNR of 15 dB. It can be seen that the average detection performance deteriorates as K increases, (the PDF moves from Rician to two-wave fading). More specifically, for $\Delta = 1$, $K = 10$ dB, a minimum SNR of 18 dB is required to achieve a $P_d = 0.9$, while for $\Delta = 1$, $K = 20$ dB and $\Delta = 1$, $K = 30$ dB a minimum SNR of 21 dB and 23 dB is required, respectively. On the other hand, ED-based spectrum sensing over Rayleigh requires an SNR of 13 dB. According to these SNR figures, it can be deduced that the SNR requirements for $P_d = 0.9$ are increased by up to 77%, which would significantly affect the energy efficiency of energy-constrained CR nodes.

Fig. 3 presents the ROC curve for ED-based spectrum sensing with up to six cooperative CR users over a TWDP fading channel with $K = 10$ dB and $\Delta = 1$ for an average SNR of $\bar{\gamma} = 5$ dB. It is shown that the detection performance of the ED-based scheme improves substantially as the number of cooperative CR users increases. The Rayleigh curve for single-user detection is provided for comparison. For this

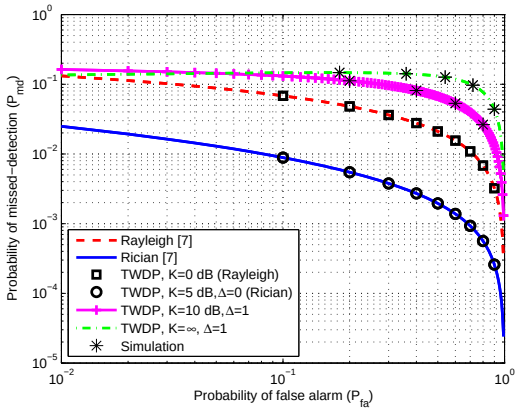

Fig. 1. Complementary ROC curves for ED-based spectrum sensing over TWDP fading with $\bar{\gamma} = 15$ dB, $u = 1$, and different K and Δ values.

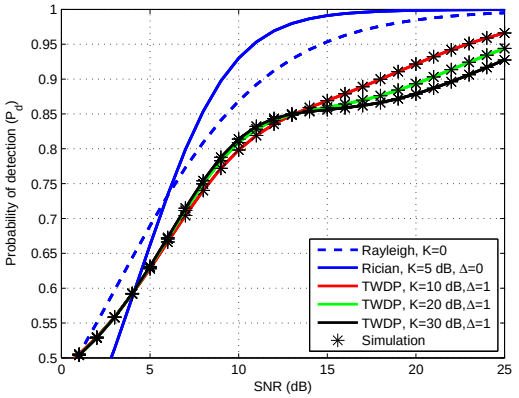

Fig. 2. $\bar{P}_{d_{TWDP}}$ versus SNR with $P_{fa} = 0.1$, $u = 1$, $\Delta = 1$, and different K values.

fading scenario and for a target probability of false alarm $P_{fa} = 0.1$, the probability of detection for six cooperative users is approximately 50% larger than for single user spectrum sensing.

Fig. 4 illustrates the detection performance for an SLS diversity scheme with up to five branches. The average SNR for each branch is set to $\bar{\gamma}_1 = 5$ dB, $\bar{\gamma}_2 = 1$ dB, $\bar{\gamma}_3 = 2$ dB, $\bar{\gamma}_4 = 3$ dB and $\bar{\gamma}_5 = 4$ dB. It can be observed that as the number of diversity branches increases, the detection performance improves by up to 38% for $L = 5$. More specifically, for a target probability of false alarm $P_{fa} = 0.1$, the probability of detection for $L = 5$ is 85% larger than the corresponding value for $L = 1$. The highest diversity gain is observed for between the no diversity case to the dual branch ($L = 2$) scheme, where an increase of 21% is observed on the average probability of detection.

Signal detection in negative SNR regions is a major challenge of spectrum sensing since ED cannot distinguish between a deeply faded primary signal and actual noise due to noise uncertainty. However, the detection performance can improve as the number of independent signal samples within an observation time interval increases. In Fig. 5 a performance analysis of ED-based spectrum sensing over TWDP in negative

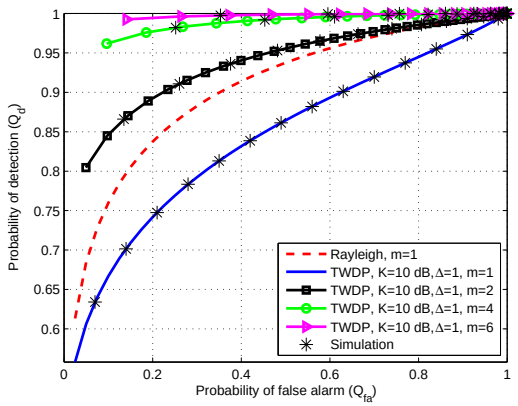

Fig. 3. ROC curves for cooperative ED-based spectrum sensing over TWDP fading for a varying number of cooperative users with, $\bar{\gamma} = 5$ dB $u = 2$, $K = 10$ dB and $\Delta = 1$.

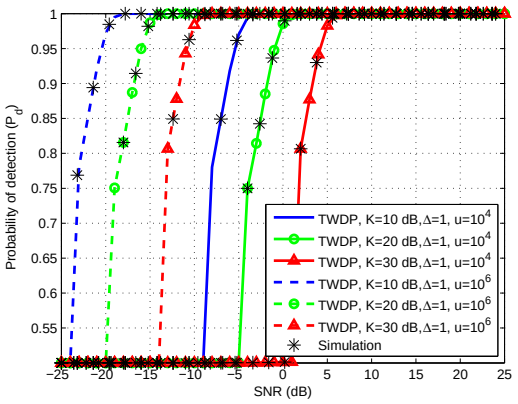

Fig. 5. $\bar{P}_{d_{TWDP}}$ versus SNR for negative SNR regions with $P_{fa} = 0.1$ and different time-bandwidth values.

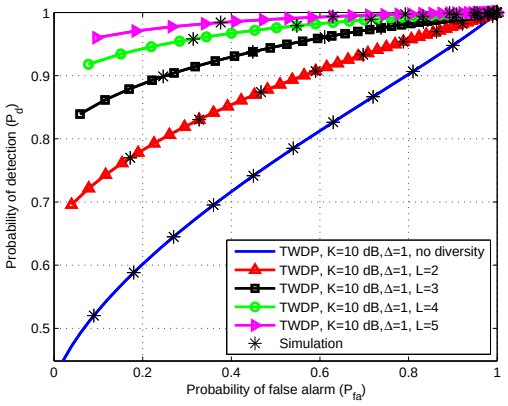

Fig. 4. ROC curves for ED-based spectrum sensing with SLS diversity reception over TWDP fading for $K = 10$ dB, $\Delta = 1$ and $\bar{\gamma}_1 = 0$ dB, $\bar{\gamma}_2 = 1$ dB, $\bar{\gamma}_3 = 2$ dB, $\bar{\gamma}_4 = 4$ dB.

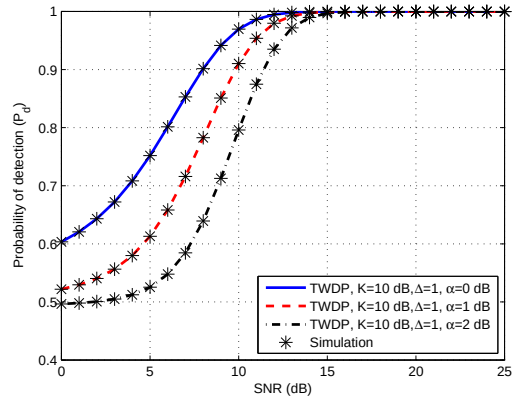

Fig. 6. $\bar{P}_{d_{TWDP}}$ versus SNR over TWDP fading with $K = 10$ dB $\Delta = 1$ and noise uncertainty for $P_{fa} = 0.1$ and $u = 10$.

SNR regions is presented. It can be seen that a gain of up to 16 dB can be achieved as u increases for a target $P_d = 0.9$ and $P_{fa} = 0.1$ for an SNR of -22 dB. It is worth noting that such time-bandwidth values may not satisfy the real-time requirements. Nevertheless, they provide an insight into the detection performance of ED-based spectrum sensing over TWDP fading channels for low SNR regions. Future research could be focused on deriving low-complexity closed-form expressions for large time-bandwidth product values by using appropriate expansions of the Bessel function for the limiting case of $u \to \infty$.

Fig. 6 shows how the detection performance varies with SNR over a TWDP fading channel with $K = 10$ dB $\Delta = 1$ under noise uncertainty. It is shown that the detection performance deteriorates as noise uncertainty increases. Indicatively, in order for ED-based spectrum sensing with $P_{fa} = 0.1$ and $u = 10$ to achieve $P_d = 0.9$ a 5 dB SNR difference is observed from $a = 0$ dB, i.e., perfect noise estimation, to $a = 2$ dB.

V. Conclusion

This article presented a comprehensive performance analysis of ED-based spectrum sensing over TWDP fading channels. A novel analytic expression for the average probability of detection over TWDP fading was derived. This expression was extended to account for SLS diversity reception and cooperative spectrum sensing. It was demonstrated that over worse than Rayleigh fading conditions, 46% and 137% higher SNR is required to achieve the same detection performance as in Rician and Rayleigh fading, respectively. To this end, it was indicated that diversity reception and cooperative spectrum sensing can significantly improve the detection performance over extreme fading conditions. Furthermore, it was shown that ED-based spectrum sensing requires large time-bandwidth product values for robust sensing in low SNR regions over TWDP. The derived expressions provide a new insight in the behavior of ED-based spectrum sensing for CR-enabled communication systems that operate under extreme fading conditions. Hence, the offered results can be used in quantifying the effects of non-conventional fading propagation environments in ED-based spectrum sensing, which can lead to improved wireless systems for emerging applications such as in-vehicular M2M communications.

APPENDIX
DERIVATION OF (14)

After expanding (14), it can be rewritten as,

$$\bar{P}_{d_{TWDP}} = e^{-\frac{\lambda}{2}} \sum_{l=0}^{u-1} \frac{\left(\frac{\lambda}{2}\right)^l}{l!} + e^{-\frac{\lambda}{2}} \sum_{n=u}^{\infty} \frac{\left(\frac{\lambda}{2}\right)^n}{n!} \left(1 - \frac{(K+1)e^{-K}}{2\bar{\gamma}} \sum_{k=0}^{n-u} \sum_{i=1}^{M} \frac{1}{k!} \times \left[e^{a_i K} \times \underbrace{\int_0^{\infty} \gamma^k e^{-\frac{K+\bar{\gamma}+1}{\bar{\gamma}}\gamma} Z(-a_i) d\gamma}_{I_-} + e^{-a_i K} \underbrace{\int_0^{\infty} \gamma^k e^{-\frac{K+\bar{\gamma}+1}{\bar{\gamma}}\gamma} Z(a_i) d\gamma}_{I_+} \right] \right). \tag{A.1}$$

With reference to (9), $I_{\pm}$ is given as,

$$I_{\pm} = \int_0^{\infty} \gamma^k e^{-\frac{K+\bar{\gamma}+1}{\bar{\gamma}}\gamma} I_0\left(2\sqrt{\frac{K(K+1)(1\pm a_i)\gamma}{\bar{\gamma}}}\right) d\gamma. \tag{A.2}$$

Based on [23, eq. (6.643-2)] for $\mu = k + \frac{1}{2}$, $\alpha = \frac{K+\bar{\gamma}+1}{\bar{\gamma}}$, $\beta = \sqrt{\frac{K(K+1)(1\pm a_i)}{\bar{\gamma}}}$, and $\nu = 0$, the solution to (A.2) is given as,

$$I_{\pm} = \frac{\Gamma(k+1)}{\Gamma(1)} \left(\sqrt{\frac{K(K+1)(1-a_i)}{\bar{\gamma}}}\right)^{-1} e^{\frac{K(K+1)(1-a_i)}{2(K+\bar{\gamma}+1)}} \times \left(\frac{K+\bar{\gamma}+1}{\bar{\gamma}}\right)^{-\left(k+\frac{1}{2}\right)} M_{-\left(k+\frac{1}{2}\right),0}\left(\frac{K(K+1)(1\pm a_i)}{K+\bar{\gamma}+1}\right), \tag{A.3}$$

where M is the Whittaker function [23].

Given the Whittaker function identity [23, eq. (9.220-2)] yields,

$$M_{-\left(k+\frac{1}{2}\right),0}\left(\frac{K(K+1)(1\pm a_i)}{K+\bar{\gamma}+1}\right) = \left(\frac{K(K+1)(1-a_i)}{K+\bar{\gamma}+1}\right)^{\frac{1}{2}} e^{-\frac{K(K+1)(1-a_i)}{K+\bar{\gamma}+1}} \Phi\left(k+1; 1; \frac{K(K+1)(1\pm a_i)}{K+\bar{\gamma}+1}\right). \tag{A.4}$$

By substituting (A.4) into (A.3) and taking into account that $\Gamma(k+1) = k!$ and $\Gamma(1) = 1$ the solution to (A.1) results in (14).

REFERENCES

[1] H. Urkowitz, "Energy detection of unknown deterministic signals,"*IEEE Proc.*, vol. 55, no. 4, pp. 523–531, Apr. 1967.

[2] V. Kostylev, "Energy detection of a signal with random amplitude," in *Proc. IEEE Int. Conf. Commun.*, vol. 3, 2002, pp. 1606–1610.

[3] J. Dong, S. Zhang, and X. Wu, "Cross-correlation processing based an energy detection algorithm for non-carrier uwb radar," in *Proc. IEEE Int. Geosci. Remote Sens.*, pp. 1537–1540, Jul. 2013.

[4] S. Haykin, D. Thomson, and J. Reed, "Spectrum sensing for cognitive radio," *IEEE Proc.*, vol. 97, no. 5, pp. 849–877, May 2009.

[5] S. Haykin, "Cognitive radio: brain-empowered wireless communications," *IEEE J. Sel. Areas Commun.*, vol. 23, no. 2, pp. 201–220, Feb. 2005.

[6] E. Chatziantoniou, B. Allen, and V. Velisavljevic, "An HMM-based spectrum occupancy predictor for energy efficient cognitive radio," in *Proc. IEEE Int. Sym. Personal, Indoor and Mobile Radio Commun.*, pp. 601–605, Sep. 2013.

[7] F. Digham, M.-S. Alouini, and M. K. Simon, "On the energy detection of unknown signals over fading channels," *IEEE Trans. Commun*, vol. 55, no. 1, pp. 21–24, Jan. 2007.

[8] S. Herath and N. Rajatheva, "Analysis of equal gain combining in energy detection for cognitive radio over nakagami channels," in *Proc. IEEE Global Telecommun. Conf.*, Nov. 2008, pp. 1–5.

[9] S. Atapattu, C. Tellambura, and H. Jiang, "Performance of an energy detector over channels with both multipath fading and shadowing," *IEEE Trans. Wireless Commun.*, vol. 9, no. 12, pp. 3662–3670, Dec. 2010.

[10] P. Sofotasios, E. Rebeiz, L. Zhang, T. Tsiftsis, D. Cabric, and S. Freear, "Energy detection based spectrum sensing over κ-μ and κ-μ extreme fading channels," *Vehicular Technology, IEEE Trans. Veh. Technol.*, vol. 62, no. 3, pp. 1031–1040, Mar. 2013.

[11] O. Akan, O. Karli, and O. Ergul, "Cognitive radio sensor networks," *IEEE Netw.*, vol. 23, no. 4, pp. 34–40, Jul. 2009.

[12] Y. Zhang, R. Yu, M. Nekovee, Y. Liu, S. Xie, and S. Gjessing, "Cognitive machine-to-machine communications: visions and potentials for the smart grid," *IEEE Netw.*, vol. 26, no. 3, pp. 6–13, May 2012.

[13] J. Frolik, "On appropriate models for characterizing hyper-rayleigh fading," *IEEE Trans. Wireless Commun.*, vol. 7, no. 12, pp. 5202–5207, Dec. 2008.

[14] I. Sen, D. Matolak, and W. Xiong, "Wireless channels that exhibit "worse than rayleigh" fading: Analytical and measurement results," in *Proc. IEEE Mil. Commun.*, Oct. 2006, pp. 1–7.

[15] J. Frolik, "A case for considering hyper-rayleigh fading channels," *IEEE Trans. Wireless Commun.*, vol. 6, no. 4, pp. 1235–1239, April 2007.

[16] E. Chatziantoniou, B. Allen, and V. Velisavljevic, "Threshold optimization for energy detection-based spectrum sensing over hyper-rayleigh fading channels," *IEEE Commun. Letters*, vol. PP, no. 99, pp. 1–1, Mar. 2015.

[17] M. Abramowitz and I. A. Stegun, *Handbook of mathematical functions: with formulas, graphs, and mathematical tables*. Courier Dover Publications, 1972, no. 55.

[18] J. Marcum, "A statistical theory of target detection by pulsed radar," 1948.

[19] G. Durgin, T. Rappaport, and D. A. De Wolf, "New analytical models and probability density functions for fading in wireless communications," *IEEE Trans. Commun.*, vol. 50, no. 6, pp. 1005–1015, Jun. 2002.

[20] R. Subadar and A. Singh, "Performance of sc receiver over twdp fading channels," *IEEE Wireless Commun. Letters*, vol. 2, no. 3, pp. 267–270, Jun. 2013.

[21] M. K. Simon and M.-S. Alouini, *Digital communication over fading channels*. John Wiley & Sons, 2005, vol. 95.

[22] D. Shnidman, "Efficient evaluation of probabilities of detection and the generalized q-function (corresp.)," *IEEE Trans. Inf. Theory*, vol. 22, no. 6, pp. 746–751, Nov. 1976.

[23] I. S. Gradshteyn and I. M. Ryzhik, *Table of integrals, series, and products*, 7th ed. New York: Academic Press, 2007.

[24] A. Ghasemi and E. Sousa, "Impact of user collaboration on the performance of sensing-based opportunistic spectrum access," in *Proc. IEEE Veh. Technol. Conf.*, Sep. 2006, pp. 1–6.

[25] D. Duan, L. Yang, and J. Principe, "Cooperative diversity of spectrum sensing for cognitive radio systems," *IEEE Trans. Signal. Process.*, vol. 58, no. 6, pp. 3218–3227, Jun. 2010.

[26] K. Letaief and W. Zhang, "Cooperative communications for cognitive radio networks," *Proc. IEEE*, vol. 97, no. 5, pp. 878–893, May 2009.

[27] E. Neasmith and N. Beaulieu, "New results on selection diversity," *IEEE Trans. Commun.*, vol. 46, no. 5, pp. 695–704, May 1998.

[28] M. Lopez-Benitez and F. Casadevall, "Signal uncertainty in spectrum sensing for cognitive radio," *IEEE Trans. Commun.*, vol. 61, no. 4, pp. 1231–1241, Apr. 2013.